Comprehensive Mutational Analysis of the BRCA1-Associated DNA Helicase and Tumor-Suppressor FANCJ/BACH1/BRIP1

Published OnlineFirst February 22, 2021; DOI: 10.1158/1541-7786.MCR-20-0828

Comprehensive Mutational Analysis of the BRCA1-Associated DNA Helicase and Tumor-Suppressor FANCJ/BACH1/BRIP1

Jennifer A. Calvo[1], Briana Fritchman[2], Desiree Hernandez[2], Nicole S. Persky[2], Cory M. Johannessen[2], Federica Piccioni[2], Brian A. Kelch[3], and Sharon B. Cantor[1]

ABSTRACT

FANCJ (BRIP1/BACH1) is a hereditary breast and ovarian cancer (HBOC) gene encoding a DNA helicase. Similar to HBOC genes, BRCA1 and BRCA2, FANCJ is critical for processing DNA inter-strand crosslinks (ICL) induced by chemotherapeutics, such as cisplatin. Consequently, cells deficient in FANCJ or its catalytic activity are sensitive to ICL-inducing agents. Unfortunately, the majority of FANCJ clinical mutations remain uncharacterized, limiting therapeutic opportunities to effectively use cisplatin to treat tumors with mutated FANCJ. Here, we sought to perform a comprehensive screen to identify FANCJ loss-of-function (LOF) mutations. We developed a FANCJ lentivirus mutation library representing approximately 450 patient–derived FANCJ nonsense and missense mutations to introduce FANCJ mutants into FANCJ knockout (K/O) HeLa cells. We performed a high-throughput screen to identify FANCJ LOF mutants that, as compared with wild-type FANCJ, fail to robustly restore resistance to ICL-inducing agents, cisplatin or mitomycin C (MMC). On the basis of the failure to confer resistance to either cisplatin or MMC, we identified 26 missense and 25 nonsense LOF mutations. Nonsense mutations elucidated a relationship between location of truncation and ICL sensitivity, as the majority of nonsense mutations before amino acid 860 confer ICL sensitivity. Further validation of a subset of LOF mutations confirmed the ability of the screen to identify FANCJ mutations unable to confer ICL resistance. Finally, mapping the location of LOF mutations to a new homology model provides additional functional information.

Implications: We identify 51 FANCJ LOF mutations, providing important classification of FANCJ mutations that will afford additional therapeutic strategies for affected patients.

Introduction

FANCJ [BRCA1-associated helicase 1, (BACH1) or BRCA1 interacting protein (BRIP1)] was identified as a direct interacting partner of BRCA1. Similar to BRCA1, FANCJ was shown to function in DNA repair and to be mutated in patients with hereditary breast cancer (1). Unlike BRCA1 or BRCA2 clinical mutations that informed little about how DNA repair and tumor suppression were mediated, mutations in the FANCJ helicase domain provided a direct connection between DNA metabolism and tumor suppression (2). Although the link between FANCJ and hereditary breast cancer suppression has been recently questioned, deleterious germline mutations in FANCJ are significantly associated with an increased risk of ovarian cancer, observed in 0.9% to 2.5% of patients with ovarian cancer (3–8). In fact, after BRCA1 and BRCA2, FANCJ is the third most common cancer susceptibility gene in ovarian cancer (5, 7, 8). In addition to hereditary breast and ovarian cancer (HBOC), FANCJ mutations are found in melanoma, prostate and hereditary colon cancers, providing evidence that FANCJ mutations may be a risk factor in multiple types of cancer (9–11). Indeed, FANCJ, BRCA1, and BRCA2 are bi-allelically mutated in Fanconi anemia (FA), a bone marrow failure disease that also predisposes to cancers such as leukemia (12).

Consistent with its roles as an ATPase, DNA helicase, and translocase, FANCJ contains a highly conserved helicase homology domain with seven conserved motifs, including Walker A and Walker B boxes, as well as an iron-sulfur (Fe-S) cluster that are all essential for its catalytic activity (see **Fig. 1A**). The DNA-dependent ATPase function of FANCJ catalytically unwinds a range of duplex DNA substrates as well as secondary DNA structures such as G-quadruplexes (G4; refs. 13–15). These DNA-unwinding activities support efficient replication and the progression of cells through S-phase, the mobilization of DNA repair protein and the activation of checkpoint responses as well as DNA repair activities during replication stress (16–20). Most notably, FANCJ catalytic activity is required for the processing of inter-strand crosslinks (ICL), which requires coordination with the mismatch repair protein, MLH1, that binds lysine residues 141 and 142 within the FANCJ helicase domain. Accordingly, loss of FANCJ catalytic activity or MLH1 binding causes exceedingly elevated sensitivity to ICL-inducing agents (21). Likewise, FA-associated FANCJ clinical mutations fail to restore ICL resistance, consistent with the role of FANCJ enzyme activity in ICL repair processing (14). Although other pathogenic variants that disrupt FANCJ enzyme function,

[1]Department of Molecular Cell and Cancer Biology, University of Massachusetts Medical School, Worcester, Massachusetts. [2]The Broad Institute of MIT and Harvard, Cambridge, Massachusetts. [3]Department of Biochemistry and Molecular Pharmacology, University of Massachusetts Medical School, Worcester, Massachusetts.

Note: Supplementary data for this article are available at Molecular Cancer Research Online (http://mcr.aacrjournals.org/).

Current address for C.M. Johannessen: Department of Oncology, Novartis Institutes of Biomedical Research, Cambridge, Massachusetts; and current address for F. Piccioni: Merck Research Laboratories, Boston, Massachusetts.

Corresponding Author: Sharon B. Cantor, Department of Molecular Cell and Cancer Biology, University of Massachusetts Medical School, 364 Plantation Street, LRB 415, Worcester MA 01605. E-mail: Sharon.Cantor@umassmed.edu

Mol Cancer Res 2021;19:1015–25

doi: 10.1158/1541-7786.MCR-20-0828

Published OnlineFirst February 22, 2021; DOI: 10.1158/1541-7786.MCR-20-0828

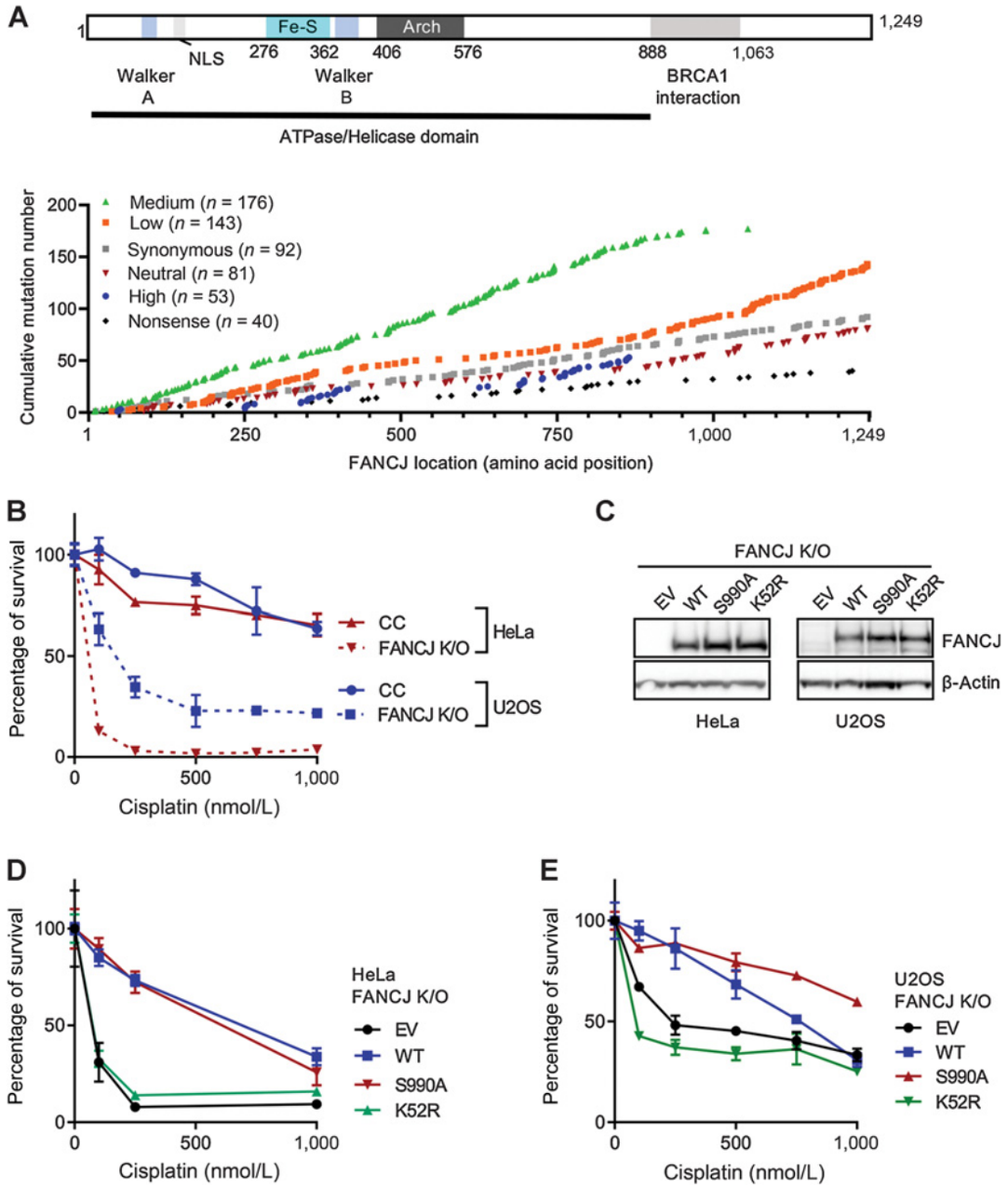

Figure 1.

The FANCJ helicase exhibits numerous mutations in cancer, with varying predictive severity, and deficiency of FANCJ or its helicase function results in severe ICL sensitivity. **A,** Schematic representation of the FANCJ protein, including Fe–S cluster, DEAH boxes, including Walker A and Walker B boxes, and the Arch domain. The 595 FANCJ mutations are aligned with the protein schematic and further classified by type of mutation; nonsense ($n = 40$), synonymous ($n = 92$), and missense mutations are further separated by their Mutation Assessor determination of high ($n = 53$), medium (176), low ($n = 143$), and neutral ($n = 81$) assessment. **B,** Cisplatin sensitivity plotted for U2OS FANCJ K/O and HeLa FANCJ K/O as compared with appropriate CRISPR controls (CC). **C,** Immunoblotting illustrating FANCJ expression following infection with FANCJ lentivirus. Cisplatin sensitivity plotted for HeLa FANCJ K/O cells (**D**) or U2OS FANCJ K/O cells (**E**) following infection with FANCJ virus lentivirus.

expression, or splicing have been identified (17, 20, 22, 23), the majority of FANCJ sequence changes remain unclassified, thereby limiting clinical utility.

There are also several protein interactions outside the helicase domain in the less conserved C-terminal region of FANCJ. Most notably, the direct interaction with BRCA1 is mediated by phosphorylation of FANCJ serine 990 (**Fig. 1A**; ref. 24). Although loss of this phosphorylation and BRCA1 binding does not sensitize to ICL-inducing agents, homologous recombination (HR) is reduced and the DNA damage tolerance mechanism of translesion synthesis (TLS) is

Published OnlineFirst February 22, 2021; DOI: 10.1158/1541-7786.MCR-20-0828

enhanced (25, 26). The phosphorylation of S990 also mediates the acetylation of lysine 1249 and its subsequent interaction with CtIP, an interaction important for DNA end resection (27, 28). Correspondingly, loss of this K1249 acetylation also disrupts HR and promotes TLS (27). FANCJ is also phosphorylated at threonine 1133 in response to replication stress, facilitating a direct interaction with TOPBP1, and promotion of an ATR-dependent checkpoint in response to replication stress (29). Additional DNA repair proteins, including MRE11, RPA, and BLM bind within the FANCJ carboxy terminus (881–1249), and although the binding parameters remain to be fully characterized, these interactions have been shown to regulate FANCJ enzyme activity (30–34). Although only MLH1 binding has been shown to be essential for ICL resistance, other FANCJ interactions, including BRCA1 and TOPBP1, modulate its DNA repair and checkpoint activities, respectively, in a manner that could be critical for tumor suppression (reviewed in ref. 35).

Here, we provide a comprehensive mutational analysis of the DNA helicase, FANCJ. We generated a library of nonsense and missense mutations obtained from the cBioPortal for Cancer Genomics and evaluated their function in a high-throughput screen (HTS) to evaluate sensitivity to ICL-inducing agents (36, 37). We observed a distinct LOF phenotype due to 51 distinct FANCJ mutations (25 nonsense and 26 missense), all of which are located within the FANCJ helicase domain (1–880). Mapping the missense mutations to a homology model of FANCJ provided additional insight to the mechanism of disruption. This new information about the functional consequences of clinically relevant FANCJ mutations will provide important insights to interpret cancer risk as well as to manage prevention and treatment strategies.

Materials and Methods

FANCJ mutations and *in silico* programs

FANCJ mutations included in the study were identified using cBioPortal (http://cbioportal. org); more information on mutations found in Supplementary Table S1 (36, 37). Negative controls included synonymous mutations at same amino acid as cBioPortal mutations as well as non-pathogenic mutations seen in healthy patients (http://gnomad.broadinstitute.org/; ref. 38). The library also contained controls spiked into the plate, including; no virus, virus expressing dsRed or eGFP, virus expressing FANCJ K52R or S990A. Missense mutations were evaluated using the following *in silico* programs, Mutation Assessor (http://mutationassessor.org/r3/; ref. 39), Polyphen-2 (http://genetics.bwh.harvard.edu/pph2/index.shtml; ref. 40), and SIFT (https://sift.bii.a-star.edu.sg/; ref. 41). Protein alignments were performed using Clustal Omega (https://www.ebi.ac.uk/Tools/msa/clustalo/; ref. 42).

Cell lines and reagents

HeLa and U2OS FANCJ K/O and CRISPR control (CC) cells (26, 43) were grown in DMEM supplemented with 10% FBS (Sigma-Aldrich) and 1% penicillin/streptomycin (Gibco). HeLa FANCJ K/O cells tested negative for *Mycoplasma* before the HTS. Cisplatin (Sigma-Aldrich) was prepared in 1 mmol/L saline solution, per the manufacturer's instructions and mitomycin C (MMC; Sigma-Aldrich) was prepared in water.

Immunoblotting

Cells were harvested, lysed, and processed for Western blot analysis as described previously using 150 mmol/L NETN lysis buffer [20 mmol/L Tris; (pH 8.0), 150 mmol/L NaCl, 1 mmol/L EDTA, 0.5% NP-40, and Halt Protease inhibitor cocktail; Thermo Fisher]. Proteins were separated using SDS–PAGE and electro-transferred to nitrocellulose membranes. Membranes were blocked in 5% not fat dry milk (NFDM) PBS/Tween and incubated with primary Ab overnight at 4°C. Antibodies for Western blot analysis included anti–β-actin (Sigma-Aldrich) and anti-FANCJ (E67). Membranes were washed, incubated with horseradish peroxidase–linked secondary Abs (Amersham) for 1 hour at room temperature, and detected by chemiluminescence (Amersham).

Lentiviral production

The mutant clones in the FANCJ mutation library were individually generated using site-directed mutagenesis (Genscript) using PMT-BRD025 FANCJ WT (wild-type) as template, and each mutant clone was sequence verified (Genscript Piscataway). Details of standard virus production pipelines can be found at the Broad Institute's Genetic Perturbation Platform website (https://portals.broadinstitute.org/gpp/public/). Viruses for the mutant and WT FANCJ were produced in 96-well plates using HEK293T cells transfected with packaging vector psPAX2 (100 ng), envelope plasmid CMV-VSVG (10 ng), and respective PMT-BRD025 FANCJ mutant plasmid (100 ng). Lentiviral-containing supernatants were harvested 31 hours post-transfection and stored in polypropylene plates at −80°C until use.

HTS conditions

Mutant and WT FANCJ virus was robotically arrayed into 2 × 384-well plates, from which virus was later transferred to cell plates. Separately, 200 HeLa FANCJ K/O cells per well were seeded into 384-well white-walled, clear-bottom plates in a volume of 40 μL. Plates were incubated at room temperature for 30 minutes to aid with even seeding within each well. Then 10 μL of media containing polybrene (4 μg/mL) and 6 μL of the arrayed lentivirus were sequentially added using the JANUS liquid handler and the plates were centrifuged for 30 minutes at 2,250 RPM (1,178 x *g*) at 37°C followed by overnight incubation at 37°C (5% CO_2). The following morning, using liquid handling, 50 μL of media were removed and replaced with 50 μL of fresh media. Cell plates were randomly divided into 6 treatment arms in duplicate: Untreated, cisplatin, and MMC. In addition, one plate was treated with puromycin with which to calculate infection efficiencies. 48 hours after infection we added 10 μL of media or drugs were added to each well of the plates to a final concentration of either: 500 nmol/L cisplatin, 10 nmol/L MMC, 0.15 μg/mL puro, or media to the untreated plates. 5 days after drug addition, cell viability was quantified through addition of 10 μL of CellTiterGlo (Promega) and subsequently read out on an EnVision Multilabel Reader (PerkinElmer). Percentage of viabilities were determined by dividing the average luminescence value in drug by the average luminescence value in the absence of drug.

Structural modeling

We used the Phyre2 server to generate a homology model of the FANCJ protein (44). The model was primarily based on structures of the FANCJ homologs XPD and DinG (45, 46). The resulting model was built with high confidence in the modeled regions and had good stereochemistry. To incorporate the FeS cluster into the complex, we superposed the XPD structure (45) onto the FANCJ model and used the coordinates of FeS cluster from the superposed XPD protein. The FeS cluster is positioned with high confidence due to the substantial sequence similarity in this region. To model how ATP and DNA bind to FANCJ, we superposed the DinG structure and used the superposed coordinates of these ligands. The ATP is positioned with high confidence due to the high conservation in the region and the well

Published OnlineFirst February 22, 2021; DOI: 10.1158/1541-7786.MCR-20-0828

understood ATPase mechanism. The DNA is placed with much less confidence, primarily because of the weaker sequence similarity in the single-stranded DNA (ssDNA)–binding groove. Therefore, the positioning of ssDNA in the resulting model should not imply confident prediction of which residues directly bind to the DNA; rather, the modeled DNA should only be used to localize the approximate location of the DNA strand.

Statistical analysis

GraphPad Prism was used to calculate correlation. For the Z factor assay, 200 HeLa FANCJ K/O cells/well in 384 plates were spinfected with 8-μL FANCJ WT or FANCJ K52R lentivirus, and 24 hours after infection, media were changed and 48 hours after infection, plates were treated with 20 nmol/L MMC. Five days after MMC treatment, survival was measured and luminescence data from 176 FANCJ WT and 176 FANCJ K52R samples were used to determine Z factor using the following equation (47):

$$Z' = 1 - [(3 \text{ SD of sample to } 3 \text{ SD of control})/ |\text{mean of sample} - \text{mean of control}|]$$

Results

Generation of a FANCJ mutation library from cancer-associated mutations

Next-generation sequencing has identified mutations throughout the FANCJ gene, but the functional consequences remain mostly unclassified. To fully examine the significance of FANCJ clinical mutations, we evaluated nonsense and missense mutations obtained from the cBioPortal for Cancer Genomics, (36, 37) the vast majority being somatic mutations (Supplementary Table S1). We generated a lentiviral expression library of 595 mutations throughout the FANCJ gene, corresponding to 40 nonsense mutations and over 460 missense mutations (**Table 1**; Supplementary Table S2). Positive controls included FANCJ K52R, a known LOF mutation that disrupts FANCJ catalytic activity (1, 48, 49), and negative controls included 92 synonymous mutations and 46 non-pathogenic mutations from healthy patients identified from Genome Aggregation Database (gnomAD; **Table 1**; ref. 38). FANCJ mutations were evenly distributed throughout the FANCJ gene product (Supplementary Fig. S1A). Evaluation of the mutations using the *in silico* mutation prediction program, Mutation Assessor, which uses evolutionary conservation of amino acids to predict functional impact of substitutions, revealed that approximately half of the mutations are classified as high or medium risk of functional impact whereas the other half are classified as low or neutral functional impact (39, 50). Similarly, additional predictive algorithms, SIFT and Polyphen-2, confirmed that approximately half of missense mutations are predicted to be deleterious whereas the other half tolerated (Supplementary Fig. S2; refs. 40, 41).

Table 1. FANCJ mutation library: description and enumeration of controls and mutations.

Controls	Number
Empty (no virus)	124
S990A (BRCA1 binding mutant)	8
K52R (LOF control)	8
dsRed or eGFP	16
FANCJ WT (control)	16
Total controls	172
Mutations	**Number**
cBioPortal	
Nonsense mutations	40
Missense mutations	396
In-frame deletion	5
cBioPortal total	441
gnomAD	
Missense mutations	28
Synonymous mutations	18
gnomAD total	46
Silent mutations	72
Additional mutations (literature)	36
Total mutations	595

Design of HTS to identify FANCJ LOF mutations

To evaluate the functional consequence of FANCJ mutants, we first identified a FANCJ-deficient cell line amenable to high-throughput screening. We took advantage of the sensitivity of FANCJ-deficient cells to ICL-inducing agents and assessed ICL sensitivity in two CRISPR–CAS9-generated FANCJ-knockout (K/O) cells lines, osteosarcoma (U2OS FANCJ K/O) and cervical adenocarcinoma (HeLa FANCJ K/O; refs. 26, 43). We observed the expected sensitivity to the ICL-inducing agents, MMC and cisplatin, in both FANCJ K/O cell lines, when compared with CCs, but the HeLa FANCJ K/O cells were distinctly more sensitive than U2OS FANCJ K/O cells (**Fig. 1B**; Supplementary Fig. S1B). We confirmed complementation with WT FANCJ conferred ICL resistance in FANCJ K/O cells. Specifically, FANCJ K/O cells were infected with virus from a lentiviral construct expressing empty vector (EV), FANCJ WT, FANCJ K52R, a known helicase-dead and LOF mutant, or FANCJ S990A, the BRCA1 interaction-defective mutant (2, 24). An immunoblot revealed lentiviral infection resulted in FANCJ expression, and sensitivity assays confirmed cisplatin resistance in cells expressing either FANCJ WT or FANCJ S990A, whereas cells expressing EV or FANCJ K52R failed to confer cisplatin resistance (**Fig. 1C–E**). Cisplatin treatment (250 nmol/L) resulted in a 9-fold difference in survival between EV and FANCJ WT in HeLa FANCJ K/O compared with <2-fold difference in survival in U2OS FANCJ K/O cells (**Fig. 1D** and **E**). We therefore exploited the larger window in the HeLa cells to maximize our ability to identify FANCJ clinical mutations with LOF phenotypes in the HTS.

Finally, to evaluate whether screening conditions were robust and suitable to identify LOF mutations, we determined the Z-factor (Z), a statistical test designed to evaluate signal range as well as data variation (47). HeLa FANCJ K/O cells were infected with either FANCJ WT or FANCJ K52R virus, treated with MMC and survival was evaluated. Although this experiment only resulted in 57% infection efficiency (IE), we obtained a $Z = 0.492$. Because a $Z \geq 0.5$ indicates assay conditions are ideal for the HTS, this test suggested that our screen conditions could provide the sufficient quality and robustness to identify LOF mutations (Supplementary Fig. S1C; ref. 47).

Identification of FANCJ LOF mutants with HTS

The HTS was performed in 384-well plates in technical duplicates under three experimental conditions; untreated, MMC, and cisplatin (**Fig. 2A**). The use of these two similar ICL-inducing agents provided orthogonal biological replicates to help increase confidence in LOF mutants. The doses of MMC (10 nmol/L) and cisplatin (500 nmol/L) were chosen as the lowest dose that provided the largest signal window between sensitivity of FANCJ K/O K52R and resistance in FANCJ K/O WT cells (Supplementary Fig. S1D). An additional condition included in the screen was puromycin treatment to assess IE; removal of clones with <50% IE prevented the incorrect classification of low expressors as

Published OnlineFirst February 22, 2021; DOI: 10.1158/1541-7786.MCR-20-0828

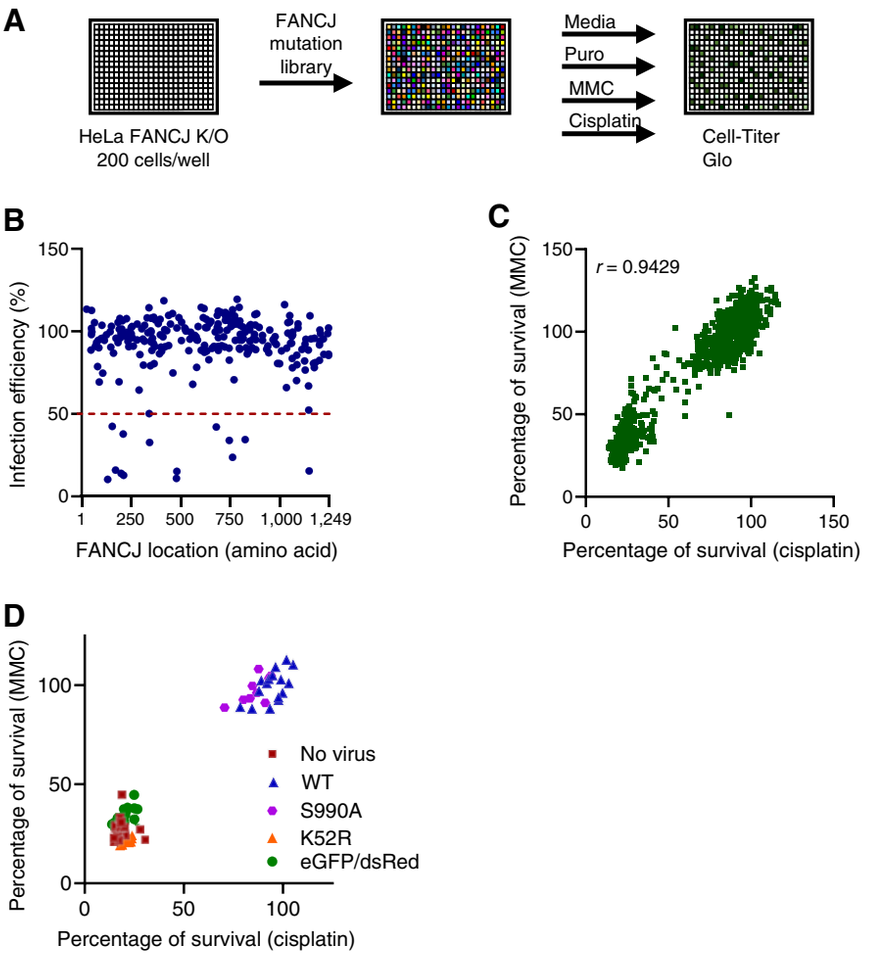

Figure 2.

High-throughput screen (HTS) of FANCJ mutations provides conditions to identify FANCJ LOF mutations. **A,** Schematic representation of HTS. HeLa FANCJ K/O (200/well) are infected with FANCJ mutation library in 384-well plates and left untreated or treated with cisplatin (500 nmol/L), MMC (10 nmol/L), or puromycin (0.15 μg/mL). Five days after treatment, survival was quantitated using Cell-Titer Glo. **B,** Infection efficiency of FANCJ mutation library is shown. Mutations ($n = 14$) found under the dotted line (<50% survival) were excluded from screen due to low infection efficiency. **C,** Correlation between cisplatin survival and MMC survival. **D,** The percentage of survival of controls to MMC and cisplatin.

LOF mutations. After exclusion of 14 mutations for low IE, we obtained sensitivity data for >97% of the mutation library, with a mean IE of >99%, indicating suitable complementation with the mutation library (**Fig. 2B**). The two technical replicates of each ICL-inducing agents exhibited close correlation (Supplementary Fig. S3A). In addition, the sensitivity of FANCJ mutants to MMC treatment correlated closely with the sensitivity to cisplatin treatment, consistent with the fact that both are ICL-inducing agents with similar mechanisms of action (**Fig. 2C**). The controls performed as expected, with cells expressing FANCJ WT or FANCJ S990A conferring resistance to ICL-inducing agents and exhibiting increased survival, and cells infected with FANCJ K52R, eGFP, dsRed or mock-infected cells failing to confer resistance to MMC or cisplatin treatment (**Fig. 2D**). Furthermore, the synonymous mutation negative controls, which result in no alteration of gene product, as well as non-pathogenic mutations from healthy individuals exhibited resistance to cisplatin and MMC treatment, indicating complementation with these presumably functional FANCJ clones conferred resistance to ICL-inducing agents in our screen (Supplementary Fig. S3B).

To determine whether the FANCJ mutations in our library had the ability to confer resistance to ICL-inducing agents when introduced into FANCJ K/O cells, we evaluated survival following treatment with cisplatin and MMC separately. Mutants unable to confer cellular resistance to ICL-inducing agents were classified as FANCJ LOF mutants using the criteria of ≤50% survival following treatment with cisplatin or MMC, as compared with untreated cells. The known LOF mutations included in the screen, as expected, were classified as the LOF mutations, including the well-characterized dominant negative helicase dead K52R mutation, as well as mutations observed in patients with FA, A349P, and H396D (20, 51). We also observed LOF in G690E, a mutation recently characterized as a null mutation (52).

Examination of the 40 nonsense mutations revealed 25 LOF nonsense mutations and elucidated a clear relationship between location of FANCJ truncation and cisplatin sensitivity. With few exceptions, a truncation before amino acid 860 resulted in cisplatin sensitivity, whereas after amino acid 860 resulted in cisplatin resistance (**Fig. 3A**; **Table 2**). This indicates that the first 860 amino acids of FANCJ, corresponding to the helicase domain, are required for the cellular resistance to ICL-inducing agents, and the C-terminal region (881–1249) of FANCJ, including the protein interaction domains located here, is dispensable for ICL resistance, reviewed in refs. 9, 14. Although the vast majority of nonsense mutations before amino acid 860 result in cisplatin sensitivity, this relationship was not absolute because three mutations (E357*, E795*, and R789*) retained the ability to confer ICL resistance (**Fig. 3A**).

Similar to the nonsense mutations, all of the missense mutations categorized as LOF mutations mapped to the first approximately 860 amino acids of FANCJ, with the vast majority in residues evolutionarily conserved between human, mouse, and chicken (**Fig. 3B**; **Table 2**; Supplementary Fig. S4). In addition, the majority of missense LOF

Published OnlineFirst February 22, 2021; DOI: 10.1158/1541-7786.MCR-20-0828

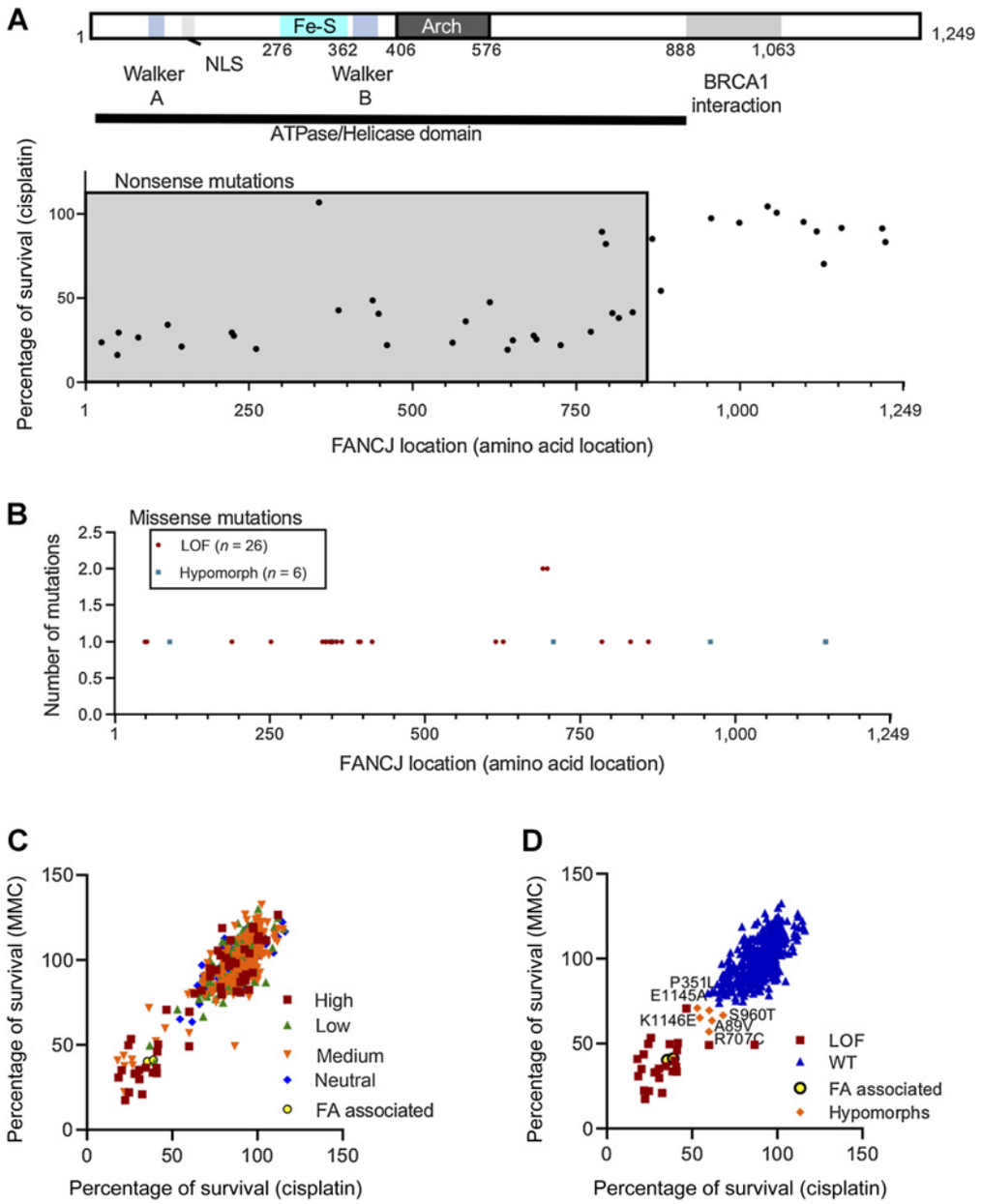

Figure 3.

FANCJ LOF mutations are localized within the helicase domain. **A,** Schematic of FANCJ protein mapping location of nonsense mutations ($n = 40$) and cisplatin sensitivity. Shaded area with reduced survival following cisplatin treatment illustrates LOF mutations are localized to first 860 amino acids. **B,** Localization of LOF or hypomorphic missense mutations, aligned to FANCJ protein schematic in **A**. **C,** The percentage of survival of entire mutation library to MMC and cisplatin. Missense mutations are categorized by their Mutation Assessor designation of high, medium, low, and neutral, and the two FA controls (A349P and H369D). **D,** The percentage of survival of missense mutations to MMC and cisplatin. Mutations are classified as WT, LOF, hypomorph, and the two FA controls (A349P and H369D).

mutations were classified as high functional impact using Mutation Assessor, deleterious using SIFT, and damaging using Polyphen-2, consistent with the clustering of the mutations primarily in the evolutionary-conserved DEAH boxes and Fe–S motifs (**Figs. 3C** and **4A**). These findings are similar to the localization of LOF mutations in another DNA damage–related helicase, BLM, which primarily localized to structural motifs within the helicase domain (53). A discrete set of six mutations were identified as FANCJ hypomorphs using the criteria of relative survival of >50% and <70%, relative to untreated. One hypomorph identified is R707C, a mutation recently characterized as having diminished dimerization and helicase processivity, as well as increased sensitivity to cisplatin (**Fig. 3D**; ref. 54).

Mapping LOF mutations onto a FANCJ homology model

To investigate how the LOF mutations could disrupt FANCJ structure and function, we built a homology model of the FANCJ

Published OnlineFirst February 22, 2021; DOI: 10.1158/1541-7786.MCR-20-0828

Table 2. FANCJ LOF and hypomorphic mutations.

LOF		Hypomorphic
Misssense	*Nonsense*	*Missense*
G49R	Q25*	A89V
K52R	G49*	P351L
S189L	G51*	R707C
T252R	E81*	S960T
W335L	Q126*	E1145A
L340R	Y147*	K1146E
V341D	G224*	
L347P	Q227*	
A349P	R261*	
C350F	E387*	
L358P	R439*	
F366S	W448*	
D393V	Y461*	
H396D	Q561*	
L415P	R581*	
S614Y	S618*	
E626K	Q645*	
G690E	S653*	
G690R	Q685*	
S697P	Q689*	
S697F	E726*	
R762P	S772*	
G763C	S805*	
P785L	Q815*	
R831K	R836*	
L860P		

protein. The Phyre2 server (44) generated a structural model using several related helicases as template, covering approximately 55% of the FANCJ sequence (**Fig. 4B**). This high-confidence model includes the ATPase, FeS cluster, and the Arch domain, but the FANCJ C-terminal region could not be accurately modeled because it is predicted to be largely intrinsically disordered.

Mapping the LOF mutations to this homology structure identified several distinct clusters of FANCJ LOF mutations that were primarily located in regions of known function. Only one mutation (S189L) mapped to the unstructured region between residues 66 and 240, and none were found in the long unstructured C-terminal tail. We classified the LOF mutations into four major classes that disrupt either the Fe cluster, the ATPase active site, ssDNA binding, or overall structure or folding (Supplementary Table S3). To test these predictions, we analyzed 13 LOF mutations identified in the primary screen that represent these four predicted functional classes.

Several mutations are predicted to perturb key catalytic residues that are highly conserved or invariant across the broad superfamily of ATPases of which FANCJ is a member (Supplementary Table S3; ref. 55). The G49R and K52R mutations alter highly conserved residues in the Walker A motif that are used to bind ATP (56), whereas D393V disrupts the invariant aspartate in the Walker B motif that is necessary for ATP hydrolysis (57). The R831K mutation disrupts a key residue for both ATPase activity and transmission of conformational changes; mutation of the equivalent "arginine finger" residue in the related BLM helicase causes loss of ATPase and helicase activities (58). Although H396D and S614Y do not disrupt highly conserved residues, their predicted proximity to the main catalytic machinery suggests these mutations also disrupt ATPase activity. Validation experiments confirm that these predicted ATPase-defective mutants indeed disrupt FANCJ function; G49R, D393V, S614Y, G690R, and L860P do not confer ICL resistance when expressed in FANCJ K/O cells (**Fig. 4C**; Supplementary Fig. S5).

Our model predicts that another class of LOF mutations will disrupt the FeS domain (Supplementary Table S3). The C350F mutation causes the loss of a cysteine residue that directly coordinates the FeS cluster, whereas mutation of the adjacent residue (A349P) is expected to distort the FeS-binding residues. Indeed, mutation of the equivalent residue in the related protein XPD abolishes FeS cluster formation and helicase activity (59). We predict that other mutations near the FeS cluster (W335L, L340R, V341D, L347P, L358P, and F366S) would destabilize the domain, leading to loss of FANCJ activity and consistent with this prediction, sensitivity assays clearly illustrate that V341D, F366S, and L347P mutations fail to confer ICL resistance (**Fig. 4C**; Supplementary Fig. S5).

A third class of mutations map to a region of FANCJ that our model predicts as a binding site for ssDNA. By superposing FANCJ on the structure of the related DinG protein bound to ssDNA (46), we approximate the positioning of the ssDNA-binding region into the groove between the two ATPase domains. Interestingly, we find that the T252R, S697P, S697F, R762P, and G763C mutations map to this region. Each of these residues are conserved in the related XPD helicase (T76, S541, R601, and G602 of XPD), suggesting a shared function. Because of their location in or near the DNA-binding cleft, we predict that these mutations disrupt the binding of FANCJ to ssDNA. Consistent with the importance of this functional domain, FANCJ mutations S697P and R762P fail to confer ICL resistance (**Fig. 4C**; Supplementary Fig. S5).

The final class of mutations is found in buried residues that are likely important for overall FANCJ structure and stability. Because most of residues reside in the hydrophobic cores of individual domains, we predict that these mutations will disrupt the folding or otherwise alter FANCJ structure (Supplementary Table S3). Residues in this class are found in domains throughout the modeled protein, including the FeS domain mutations (V341D, L347P, and L358P), the ATPase domain 1 (F366S), the Arch domain (L415P), and ATPase domain 2 (G690E/R, P785L, and L860P), and by the disruption of these domains, interfere with their function. It is likely that the mutations in this class disrupt FANCJ function through varied molecular mechanisms, such as reduced protein half-life or altered protein structure or dynamics. We found that the FANCJ mutants chosen for validation exhibit similar expression compared with WT FANCJ (**Fig. 4D**), indicating that the mutations do not grossly perturb levels of FANCJ. Nevertheless, the functional consequence of this class of mutations was confirmed by the failure to confer ICL resistance by the V341D, L347P, F366S, G690R, and L860P FANCJ mutants (**Fig. 4C**; Supplementary Fig. S5).

Discussion

To leverage genomic information obtained in the past decades for therapeutics and diagnostics, understanding the functional consequences of genetic variations will be critical (60). Mutations in FANCJ have been associated with HBOC for years, but the physiological consequences of the majority of FANCJ mutations still remain unclear. Our comprehensive screen provides an important step in elucidating the physiological consequences of FANCJ mutations, specifically in terms of sensitivity to ICL-inducing agents. We identified 25 nonsense and 26 missense FANCJ mutations exhibiting LOF phenotypes following treatment with DNA cross-linking agents. The majority of

Published OnlineFirst February 22, 2021; DOI: 10.1158/1541-7786.MCR-20-0828

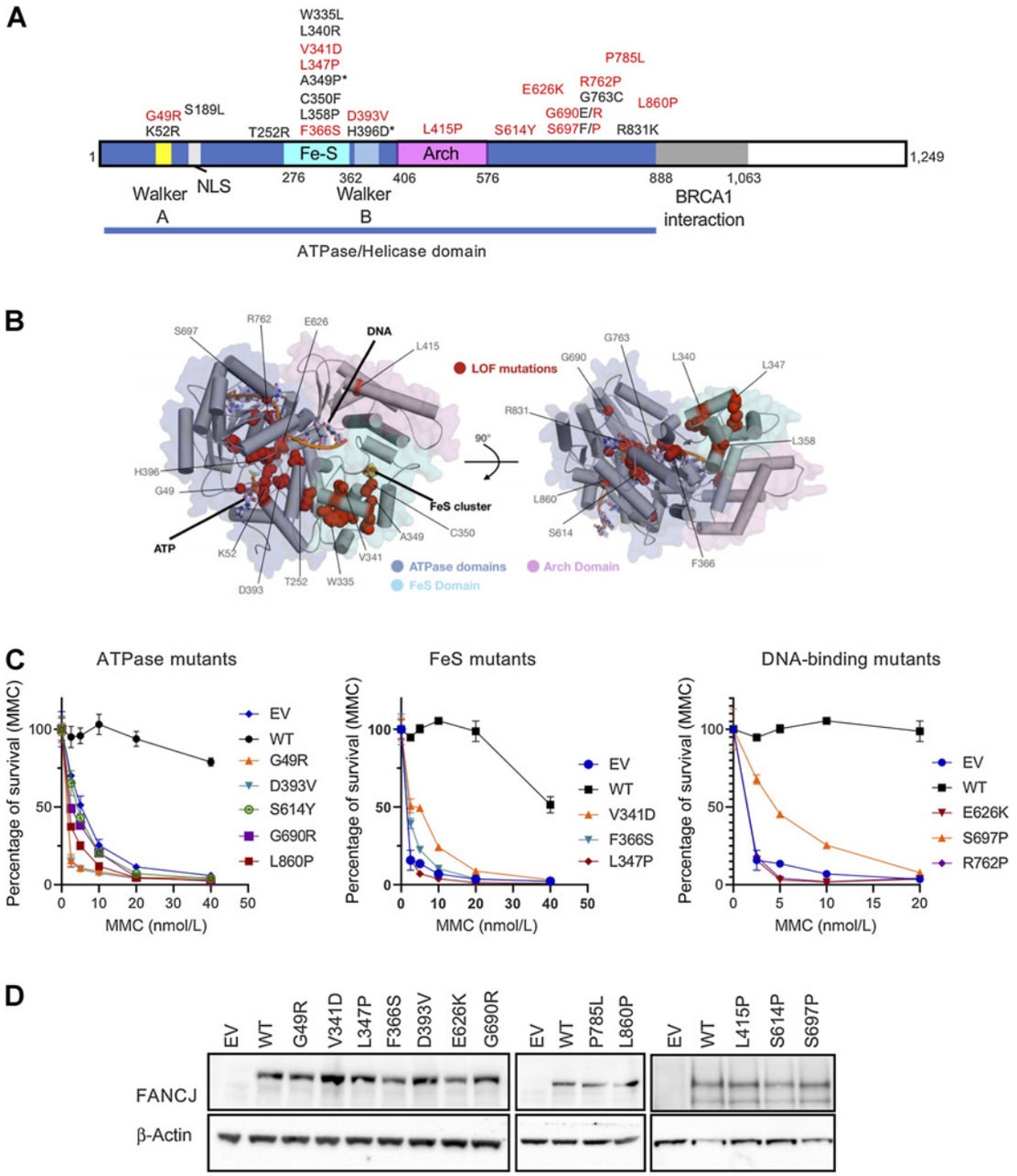

Figure 4.

FANCJ HTS identifies LOF mutations, localized in highly conserved regions. **A,** The location of the 26 FANCJ LOF missense mutations identified from screen is mapped to the FANCJ protein. FA-associated mutations are marked with an asterisk and mutations chosen for further validation are red. **B,** The homology model of the FANCJ protein illustrating the location of the LOF mutations; model is shown in two orientations. **C,** MMC sensitivity shown for HeLa FANCJ K/O cells infected with lentivirus-expressing mutants predicted to disrupt ATPase domain, the FeS cluster, or DNA-binding domain. The same WT and EV control data are shown in each plot. **D,** Immunoblotting illustrates FANCJ expression following infection of lentivirus-expressing EV, FANCJ WT, or FANCJ mutants.

these LOF mutations are located in evolutionarily conserved amino acids, constrained to the first 860 amino acids of FANCJ, and positioned in domains important for DNA helicase activity including ATPase domains and the Fe–S motif. The absence of LOF mutations in the C-terminal region (residues 881–1249) suggests that the FANCJ N-terminal helicase domain is essential for tumor suppression and that C-terminal interactions with BRCA1, BLM, TOPBP1, and CtIP instead modulate this activity (14).

Our development of a FANCJ homology model and subsequent mapping of the identified LOF mutations facilitated their categorization into four classes of disrupted function; mutations that disrupt the Fe cluster, the ATPase active site, ssDNA binding, or overall structure

or folding. The finding that rather than being randomly arranged throughout the protein, the LOF mutations are preferentially located in known regions essential for ICL resistance provides an important validation of the screen. Furthermore, the categorization of LOF mutations into functional classes may provide important insight about the functional severity of a mutation. For example, a DNA-binding mutant would be expected to be less detrimental than a mutant capable of binding DNA but unable to translocate DNA. This type of mutation was described recently in FeS cluster mutations and indeed exhibited greater MMC sensitivity compared with FANCJ K/O cells (23). Other FANCJ mutations with similar impairment (K52R and A349P) have been shown to behave as a dominant negative (2, 51). Providing additional information about potential dominant negative mutations is especially relevant given that this mutation screen examines the consequence of FANCJ mutations in a FANCJ-deficient background. Therefore, the functional impact of the identified LOF variants, and any potential actionability, will likely require homozygosity, another impairment of the WT FANCJ allele, or a dominant negative mutation.

Our screen determined that approximately 12% of clinically relevant FANCJ mutations result in a LOF phenotype, suggesting that the vast majority of clinical mutations do not alter the ability of FANCJ to confer cellular resistance to ICL-inducing agents. These results are comparable with the low frequency (11%) of BRCA1 mutations that exhibited cisplatin sensitivity in a large-scale mutation complementation assay (61). Similarly, in a recent study, only 30% of 20 mutations in FANCJ were designated null (52). However, deleterious effects (null or hypomorph phenotypes) were found in 75% of FANCJ mutations analyzed, possibly reflecting experimental differences such as higher MMC doses (52).

The low frequency of LOF mutations in our screen has several implications. For one, sensitivity to ICL-inducing agents may not be the optimal predictor of LOF. Instead, cancer-associated FANCJ mutations may result in disruption of disparate functions of FANCJ such as G4 resolution, stabilization of microsatellites, or regulation of replication stress (14, 35, 43, 62, 63). Roles for FANCJ have been identified in the suppression of HR-associated gene duplication/amplification through recruitment of CtIP to damaged sites and promotion of DNA end resection (27, 28). These numerous functions provide additional potential mechanisms by which FANCJ mutations may result in pathological phenotypes without exhibiting sensitivity to ICL-inducing agents. An important next step will be to elucidate other consequences of FANCJ mutations that retain cellular resistance to ICL-inducing agents. Performing the mutation screen under conditions that interrogate replication stress response, G4 resolution, or other FANCJ functions would likely identify additional LOF mutations.

Additional alterations to our screening parameters would likely identify FANCJ gain-of-function (GOF) mutants. As designed, the screen conditions precluded the identification of GOF mutants, which exhibited greater ICL resistance than FANCJ WT. However, this will be an important future direction because evidence suggests that the existence of FANCJ GOF mutations can promote chemoresistance and additional oncogenic properties. Consistent with this idea, the first two FANCJ helicase mutations identified in patients with hereditary breast cancer suggested that strict regulation of FANCJ-unwinding activity is important for tumor suppression; FANCJ P47A reduced ATPase/unwinding activity whereas FANCJ M299I enhanced this activity (2, 64). Moreover, mutations that disrupt BRCA1 binding (S990A mutation) or acetylation (K1249A mutation), although not currently clinically observed, shift replication toward TLS at the expense of HR, resulting in hyper-resistance to ICL-inducing agents (25, 27). Moreover, we recently demonstrated that TLS counters replication stress from genotoxins as well as oncogenes to limit replication gaps and consequently TLS is an adaptation present in many cancer cell lines (26). Higher levels of unregulated FANCJ could be fundamental to this adaptation as non-redundant studies from cBioPortal cancer datasets (36, 37) reveal that 15% of tumors show an increase in FANCJ copy number, suggesting that FANCJ expression is elevated in a range of cancers, consistent with a recent finding that increased FANCJ expression is correlated with poor patient outcomes (65, 66).

In summary, our development of a comprehensive patient-derived library of FANCJ mutations will be crucial to establish the mechanisms of pathogenicity of FANCJ mutations, because many mutations have, thus far, remained uncharacterized. Our study is especially relevant because FANCJ is often included in multigene hereditary cancer panel testing. This and other ongoing studies investigating the functional consequences of mutations in HBOC genes will allow for improved screening, prevention, and specific targeted therapeutic strategies.

Authors' Disclosures

C.M. Johannessen reports employment with Novartis Institutes for Biomedical Research. F. Piccioni reports employment with Merck Research Laboratories. No disclosures were reported by the other authors.

Authors' Contributions

J.A. Calvo: Conceptualization, validation, investigation, visualization, writing–original draft, writing–review and editing. **B. Fritchman:** Investigation, methodology. **D. Hernandez:** Investigation, methodology. **N.S. Persky:** Investigation, methodology. **C.M. Johannessen:** Conceptualization, methodology, project administration. **F. Piccioni:** Conceptualization, methodology. **B.A. Kelch:** Investigation, methodology, writing–review and editing. **S.B. Cantor:** Conceptualization, resources, supervision, funding acquisition, writing–original draft, project administration, writing–review and editing.

Acknowledgments

We thank the members of the Cantor Laboratory for helpful discussions and critical reading of the article. We thank the University of Massachusetts Medical School RNAi Core Facility for technical assistance. This research was funded by grant numbers: NIH R01 CA225018 (S. Cantor) and NIH R01 CA225018 (S. Cantor).

The costs of publication of this article were defrayed in part by the payment of page charges. This article must therefore be hereby marked *advertisement* in accordance with 18 U.S.C. Section 1734 solely to indicate this fact.

Received October 9, 2020; revised January 27, 2021; accepted February 18, 2021; published first February 22, 2021.

References

1. Cantor SB, Bell DW, Ganesan S, Kass EM, Drapkin R, Grossman S, et al. BACH1, a novel helicase-like protein, interacts directly with BRCA1 and contributes to its DNA repair function. Cell 2001;105:149–60.
2. Cantor S, Drapkin R, Zhang F, Lin Y, Han J, Pamidi S, et al. The BRCA1-associated protein BACH1 is a DNA helicase targeted by clinically relevant inactivating mutations. Proc Natl Acad Sci U S A 2004;101:2357–62.
3. Easton DF, Lesueur F, Decker B, Michailidou K, Li J, Allen J, et al. No evidence that protein truncating variants in BRIP1 are associated with breast cancer risk: implications for gene panel testing. J Med Genet 2016;53:298–309.
4. Couch FJ, Shimelis H, Hu C, Hart SN, Polley EC, Na J, et al. Associations between cancer predisposition testing panel genes and breast cancer. JAMA Oncol 2017;3:1190–6.

5. Weber-Lassalle N, Hauke J, Ramser J, Richters L, Gross E, Blumcke B, et al. BRIP1 loss-of-function mutations confer high risk for familial ovarian cancer, but not familial breast cancer. Breast Cancer Res 2018;20:7.
6. Walsh T, Casadei S, Lee MK, Pennil CC, Nord AS, Thornton AM, et al. Mutations in 12 genes for inherited ovarian, fallopian tube, and peritoneal carcinoma identified by massively parallel sequencing. Proc Natl Acad Sci U S A 2011;108:18032–7.
7. Ramus SJ, Song H, Dicks E, Tyrer JP, Rosenthal AN, Intermaggio MP, et al. Germline mutations in the BRIP1, BARD1, PALB2, and NBN genes in women with ovarian cancer. J Natl Cancer Inst 2015;107:djv214.
8. Norquist BM, Harrell MI, Brady MF, Walsh T, Lee MK, Gulsuner S, et al. Inherited mutations in women with ovarian carcinoma. JAMA Oncol 2016;2: 482–90.
9. Cantor SB, Guillemette S. Hereditary breast cancer and the BRCA1-associated FANCJ/BACH1/BRIP1. Future Oncol 2011;7:253–61.
10. Paulo P, Maia S, Pinto C, Pinto P, Monteiro A, Peixoto A, et al. Targeted next-generation sequencing identifies functionally deleterious germline mutations in novel genes in early-onset/familial prostate cancer. PLoS Genet 2018;14: e1007355.
11. Ali M, Delozier CD, Chaudhary U. BRIP-1 germline mutation and its role in colon cancer: presentation of two case reports and review of literature. BMC Med Genet 2019;20:75.
12. Datta A, Brosh RM Jr. Holding all the cards-how fanconi anemia proteins deal with replication stress and preserve genomic stability. Genes 2019;10:170.
13. Bharti SK, Sommers JA, George F, Kuper J, Hamon F, Shin-ya K, et al. Specialization among iron-sulfur cluster helicases to resolve G-quadruplex DNA structures that threaten genomic stability. J Biol Chem 2013;288:28217–29.
14. Brosh RM Jr, Cantor SB. Molecular and cellular functions of the FANCJ DNA helicase defective in cancer and in Fanconi anemia. Front Genet 2014; 5:372.
15. Lansdorp P, van Wietmarschen N. Helicases FANCJ, RTEL1 and BLM Act on guanine quadruplex DNA in vivo. Genes 2019;10:870.
16. Kumaraswamy E, Shiekhattar R. Activation of BRCA1/BRCA2-associated helicase BACH1 is required for timely progression through S phase. Mol Cell Biol 2007;27:6733–41.
17. Sarkies P, Murat P, Phillips LG, Patel KJ, Balasubramanian S, Sale JE. FANCJ coordinates two pathways that maintain epigenetic stability at G-quadruplex DNA. Nucleic Acids Res 2012;40:1485–98.
18. Schwab RA, Nieminuszczy J, Shin-Ya K, Niedzwiedz W. FANCJ couples replication past natural fork barriers with maintenance of chromatin structure. J Cell Biol 2013;201:33–48.
19. Bharti SK, Awate S, Banerjee T, Brosh RM. Getting ready for the dance: FANCJ irons out DNA wrinkles. Genes 2016;7:31.
20. Guo M, Vidhyasagar V, Talwar T, Kariem A, Wu Y. Mutational analysis of FANCJ helicase. Methods 2016;108:118–29.
21. Peng M, Litman R, Xie J, Sharma S, Brosh RM Jr, Cantor SB. The FANCJ/MutLalpha interaction is required for correction of the cross-link response in FA-J cells. Embo J 2007;26:3238–49.
22. Velazquez C, Esteban-Cardenosa EM, Lastra E, Abella LE, de la Cruz V, Lobaton CD, et al. Unraveling the molecular effect of a rare missense mutation in BRIP1 associated with inherited breast cancer. Mol Carcinog 2019;58:156–60.
23. Odermatt DC, Lee WTC, Wild S, Jozwiakowski SK, Rothenberg E, Gari K. Cancer-associated mutations in the iron-sulfur domain of FANCJ affect G-quadruplex metabolism. PLoS Genet 2020;16:e1008740.
24. Yu X, Chini CC, He M, Mer G, Chen J. The BRCT domain is a phospho-protein binding domain. Science 2003;302:639–42.
25. Xie J, Litman R, Wang S, Peng M, Guillemette S, Rooney T, et al. Targeting the FANCJ–BRCA1 interaction promotes a switch from recombination to poleta-dependent bypass. Oncogene 2010;29:2499–508.
26. Nayak S, Calvo JA, Cong K, Peng M, Berthiaume E, Jackson J, et al. Inhibition of the translesion synthesis polymerase REV1 exploits replication gaps as a cancer vulnerability. Sci Adv 2020;6:eaaz7808.
27. Xie J, Peng M, Guillemette S, Quan S, Maniatis S, Wu Y, et al. FANCJ/BACH1 acetylation at lysine 1249 regulates the DNA damage response. PLos Genet 2012; 8:e1002786.
28. Nath S, Nagaraju G. FANCJ helicase promotes DNA end resection by facilitating CtIP recruitment to DNA double-strand breaks. PLoS Genet 2020;16:e1008701.
29. Gong Z, Kim JE, Leung CC, Glover JN, Chen J. BACH1/FANCJ acts with TopBP1 and participates early in DNA replication checkpoint control. Mol Cell 2010;37:438–46.
30. Suhasini AN, Brosh RM Jr. Fanconi anemia and Bloom's syndrome crosstalk through FANCJ-BLM helicase interaction. Trends Genet 2012;28:7–13.
31. Suhasini AN, Sommers JA, Mason AC, Voloshin ON, Camerini-Otero RD, Wold MS, et al. FANCJ helicase uniquely senses oxidative base damage in either strand of duplex DNA and is stimulated by replication protein A to unwind the damaged DNA substrate in a strand-specific manner. J Biol Chem 2009;284:18458–70.
32. Suhasini AN, Sommers JA, Muniandy PA, Coulombe Y, Cantor SB, Masson J-Y, et al. Fanconi anemia group J helicase and MRE11 nuclease interact to facilitate the DNA damage response. Mol Cell Biol 2013;33:2212–27.
33. Gupta R, Sharma S, Sommers JA, Kenny MK, Cantor SB, Brosh RM Jr. FANCJ (BACH1) helicase forms DNA damage inducible foci with replication protein A and interacts physically and functionally with the single-stranded DNA-binding protein. Blood 2007;110:2390–8.
34. Dhar S, Brosh RM. BLM's balancing act and the involvement of FANCJ in DNA repair. Cell Cycle 2018;17:2207–20.
35. Cantor SB, Nayak S. FANCJ at the FORK. Mutat Res 2016;788:7–11.
36. Cerami E, Gao J, Dogrusoz U, Gross BE, Sumer SO, Aksoy BA, et al. The cBio cancer genomics portal: an open platform for exploring multidimensional cancer genomics data. Cancer Discov 2012;2:401–4.
37. Gao J, Aksoy BA, Dogrusoz U, Dresdner G, Gross B, Sumer SO, et al. Integrative analysis of complex cancer genomics and clinical profiles using the cBioPortal. Sci Signal 2013;6:pl1.
38. Karczewski KJ, Francioli LC, Tiao G, Cummings BB, Alfoldi J, Wang Q, et al. The mutational constraint spectrum quantified from variation in 141,456 humans. Nature 2020;581:434–43.
39. Reva B, Antipin Y, Sander C. Predicting the functional impact of protein mutations: application to cancer genomics. Nucleic Acids Res 2011;39:e118.
40. Adzhubei IA, Schmidt S, Peshkin L, Ramensky VE, Gerasimova A, Bork P, et al. A method and server for predicting damaging missense mutations. Nat Methods 2010;7:248–9.
41. Sim NL, Kumar P, Hu J, Henikoff S, Schneider G, Ng PC. SIFT web server: predicting effects of amino acid substitutions on proteins. Nucleic Acids Res 2012;40:W452–7.
42. Sievers F, Wilm A, Dineen D, Gibson TJ, Karplus K, Li W, et al. Fast, scalable generation of high-quality protein multiple sequence alignments using Clustal Omega. Mol Syst Biol 2011;7:539.
43. Peng M, Cong K, Panzarino NJ, Nayak S, Calvo J, Deng B, et al. Opposing roles of FANCJ and HLTF protect forks and restrain replication during stress. Cell Rep 2018;24:3251–61.
44. Kelley LA, Sternberg MJ. Protein structure prediction on the Web: a case study using the Phyre server. Nat Protoc 2009;4:363–71.
45. Greber BJ, Toso DB, Fang J, Nogales E. The complete structure of the human TFIIH core complex. Elife 2019;8:e44771.
46. Cheng K, Wigley DB. DNA translocation mechanism of an XPD family helicase. Elife 2018;7:e42400.
47. Zhang JH, Chung TD, Oldenburg KR. A simple statistical parameter for use in evaluation and validation of high-throughput screening assays. J Biomol Screen 1999;4:67–73.
48. Levran O, Attwooll C, Henry RT, Milton KL, Neveling K, Rio P, et al. The BRCA1-interacting helicase BRIP1 is deficient in Fanconi anemia. Nat Genet 2005;37:931–3.
49. Chandrasekharappa SC, Lach FP, Kimble DC, Kamat A, Teer JK, Donovan FX, et al. Massively parallel sequencing, aCGH, and RNA-Seq technologies provide a comprehensive molecular diagnosis of Fanconi anemia. Blood 2013;121: e138–48.
50. Reva B, Antipin Y, Sander C. Determinants of protein function revealed by combinatorial entropy optimization. Genome Biol 2007;8:R232.
51. Wu Y, Sommers JA, Suhasini AN, Leonard T, Deakyne JS, Mazin AV, et al. Fanconi anemia group J mutation abolishes its DNA repair function by uncoupling DNA translocation from helicase activity or disruption of protein-DNA complexes. Blood 2010;116:3780–91.
52. Moyer CL, Ivanovich J, Gillespie JL, Doberstein R, Radke MR, Richardson ME, et al. Rare BRIP1 missense alleles confer risk for ovarian and breast cancer. Cancer Res 2020;80:857–67.
53. Mirzaei H, Schmidt KH. Non-Bloom syndrome-associated partial and total loss-of-function variants of BLM helicase. Proc Natl Acad Sci U S A 2012;109: 19357–62.
54. Bharti SK, Sommers JA, Awate S, Bellani MA, Khan I, Bradley L, et al. A minimal threshold of FANCJ helicase activity is required for its response to replication stress or double-strand break repair. Nucleic Acids Res 2018;46:6238–56.

55. Leipe DD, Koonin EV, Aravind L. Evolution and classification of P-loop kinases and related proteins. J Mol Biol 2003;333:781–815.
56. Saraste M, Sibbald PR, Wittinghofer A. The P-loop—a common motif in ATP- and GTP-binding proteins. Trends Biochem Sci 1990;15:430–4.
57. Gorbalenya AE, Koonin EV, Donchenko AP, Blinov VM. Two related superfamilies of putative helicases involved in replication, recombination, repair and expression of DNA and RNA genomes. Nucleic Acids Res 1989;17: 4713–30.
58. Ren H, Dou SX, Rigolet P, Yang Y, Wang PY, Amor-Gueret M, et al. The arginine finger of the Bloom syndrome protein: its structural organization and its role in energy coupling. Nucleic Acids Res 2007;35:6029–41.
59. Rudolf J, Makrantoni V, Ingledew WJ, Stark MJ, White MF. The DNA repair helicases XPD and FancJ have essential iron-sulfur domains. Mol Cell 2006;23: 801–8.
60. Green ED, Gunter C, Biesecker LG, Di Francesco V, Easter CL, Feingold EA, et al. Strategic vision for improving human health at the forefront of genomics. Nature 2020;586:683–92.
61. Bouwman P, van der Heijden I, van der Gulden H, de Bruijn R, Braspenning ME, Moghadasi S, et al. Functional categorization of BRCA1 variants of uncertain clinical significance in homologous recombination repair complementation assays. Clin Cancer Res 2020;26:4559–68.
62. Matsuzaki K, Borel V, Adelman CA, Schindler D, Boulton SJ. FANCJ suppresses microsatellite instability and lymphomagenesis independent of the Fanconi anemia pathway. Genes Dev 2015;29:2532–46.
63. Wu Y, Suhasini AN, Brosh RM Jr. Welcome the family of FANCJ-like helicases to the block of genome stability maintenance proteins. Cell Mol Life Sci 2009;66: 1209–22.
64. Gupta R, Sharma S, Doherty KM, Sommers JA, Cantor SB, Brosh RM Jr. Inhibition of BACH1 (FANCJ) helicase by backbone discontinuity is overcome by increased motor ATPase or length of loading strand. Nucleic Acids Res 2006; 34:6673–83.
65. Gupta I, Ouhtit A, Al-Ajmi A, Rizvi SGA, Al-Riyami H, Al-Riyami M, et al. BRIP1 overexpression is correlated with clinical features and survival outcome of luminal breast cancer subtypes. Endocr Connect 2018;7:65–77.
66. Moes-Sosnowska J, Rzepecka IK, Chodzynska J, Dansonka-Mieszkowska A, Szafron LM, Balabas A, et al. Clinical importance of FANCD2, BRIP1, BRCA1, BRCA2 and FANCF expression in ovarian carcinomas. Cancer Biol Ther 2019; 20:843–54.

Published OnlineFirst February 22, 2021; DOI: 10.1158/1541-7786.MCR-20-0828

Molecular Cancer Research

Comprehensive Mutational Analysis of the BRCA1-Associated DNA Helicase and Tumor-Suppressor FANCJ/BACH1/BRIP1

Jennifer A. Calvo, Briana Fritchman, Desiree Hernandez, et al.

Mol Cancer Res 2021;19:1015-1025. Published OnlineFirst February 22, 2021.